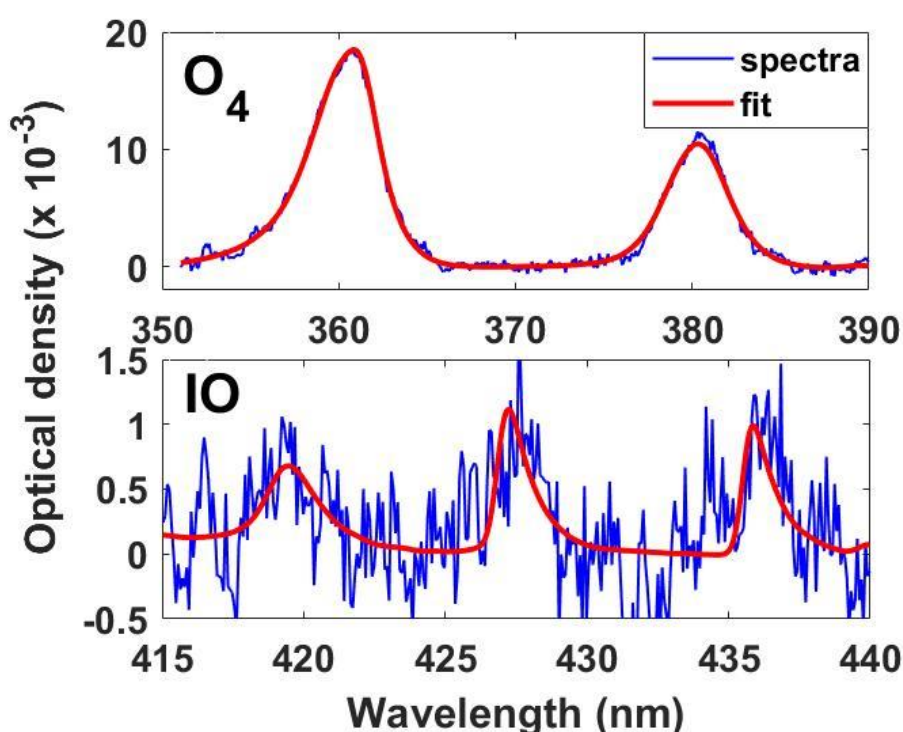


1 **Supplementary text:**

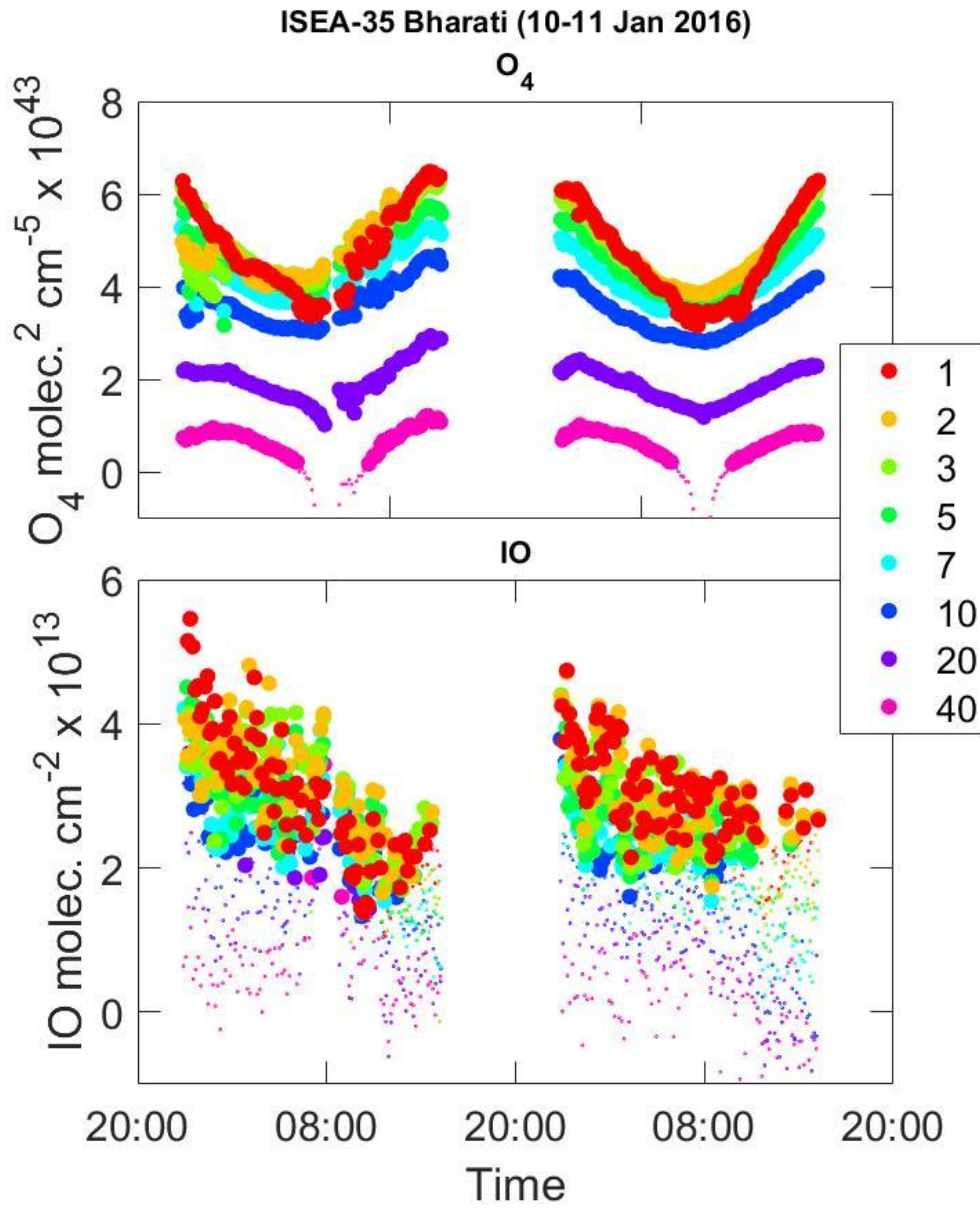
2 **Observations of iodine monoxide over three summers at the Indian Antarctic bases, Bharati**  
3 **and Maitri**

4 Anoop S. Mahajan<sup>1\*</sup>, Mriganka S. Biswas<sup>1,2</sup>, Steffen Beirle<sup>3</sup>, Thomas Wagner<sup>3</sup>, Anja Schönhardt<sup>4</sup>

5 Nuria Benavent<sup>5</sup>, and Alfonso Saiz-Lopez<sup>5</sup>



6  
7 **Figure S1:** Typical examples of DOAS fits for O<sub>4</sub> and IO are shown. Both the fits are from 1<sup>st</sup>  
8 February 2016, during ISEA-35 at Bharati at 05:33:56 UTC, solar zenith angle: 54.15° and  
9 elevation angle: 3°. The RMS for the O<sub>4</sub> window was  $4.44 \times 10^{-4}$  ( $2\sigma$  detection limit:  $0.19 \times 10^{43}$   
10 molecule<sup>2</sup> cm<sup>-5</sup>) and the retrieved DSCD was  $4.40 \pm 0.03 \times 10^{43}$  molecule<sup>2</sup> cm<sup>-5</sup>. The RMS for the  
11 IO window was  $3.7 \times 10^{-4}$  ( $2\sigma$  detection limit:  $2.11 \times 10^{13}$  molecules cm<sup>-2</sup>) and the retrieved DSCD  
12 was  $4.1 \pm 0.5 \times 10^{13}$  molecules cm<sup>-2</sup>.



13

14 **Figure S2:** A zoomed in view of two typical days, which were mostly clear, for the  $O_4$  and IO  
 15 DSCDs observed during the 35<sup>th</sup> ISEA at Bharati are shown. The smaller circles represent values  
 16 below the  $2\sigma$  detection limit of the instrument, while the bigger circles are values above the  $2\sigma$   
 17 detection limit. The data are color-coded according to elevation angles.

18

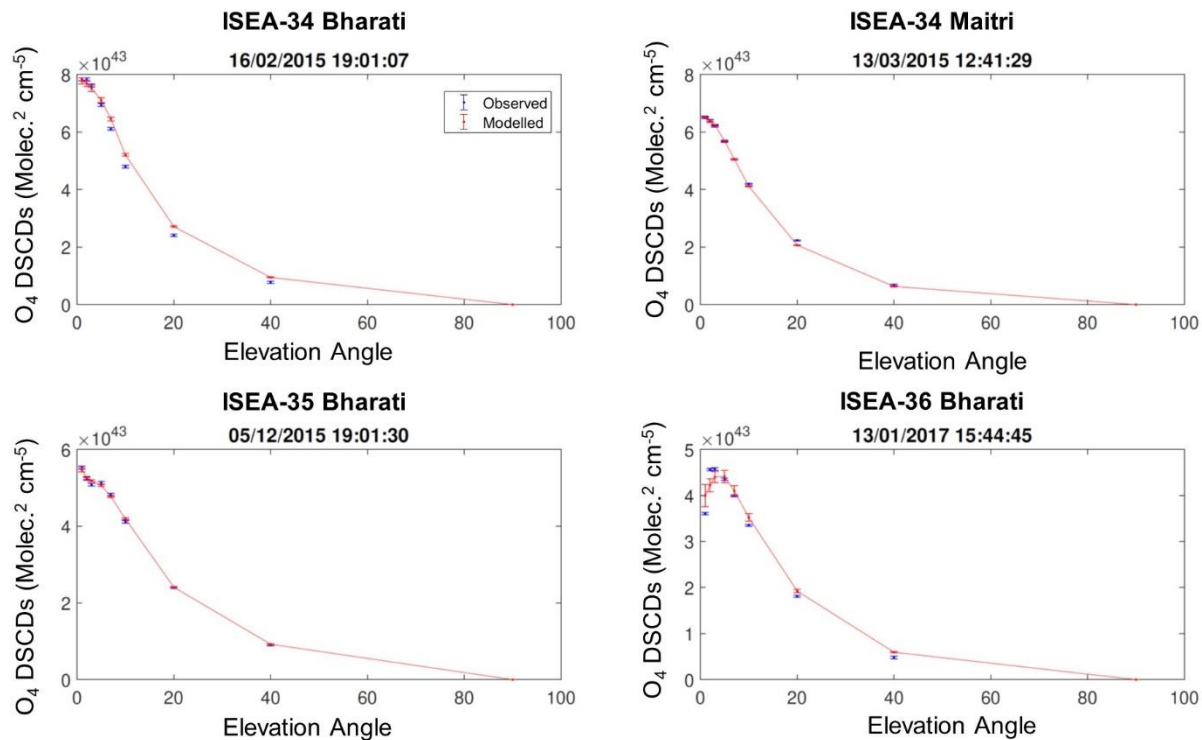


**Figure S3:** A comparison of the MAX-DOAS observed O<sub>4</sub> DSCDs with the MAPA modelled DSCDs for all the four campaigns are shown. These are typical examples chosen randomly for the scans which were retrieved as ‘good’.

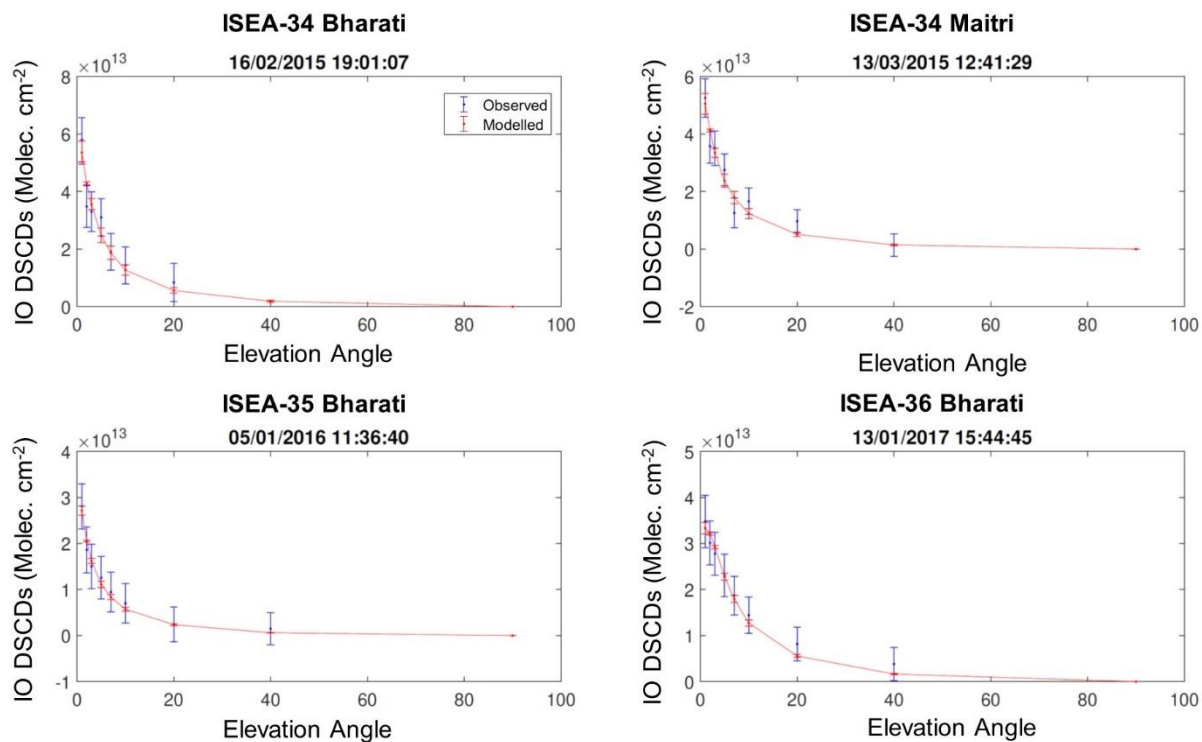


**Figure S4:** A comparison of the MAX-DOAS observed IO DSCDs with the MAPA modelled DSCDs for all the four campaigns are shown. These are typical examples chosen randomly for the scans which were scanned as ‘good’.

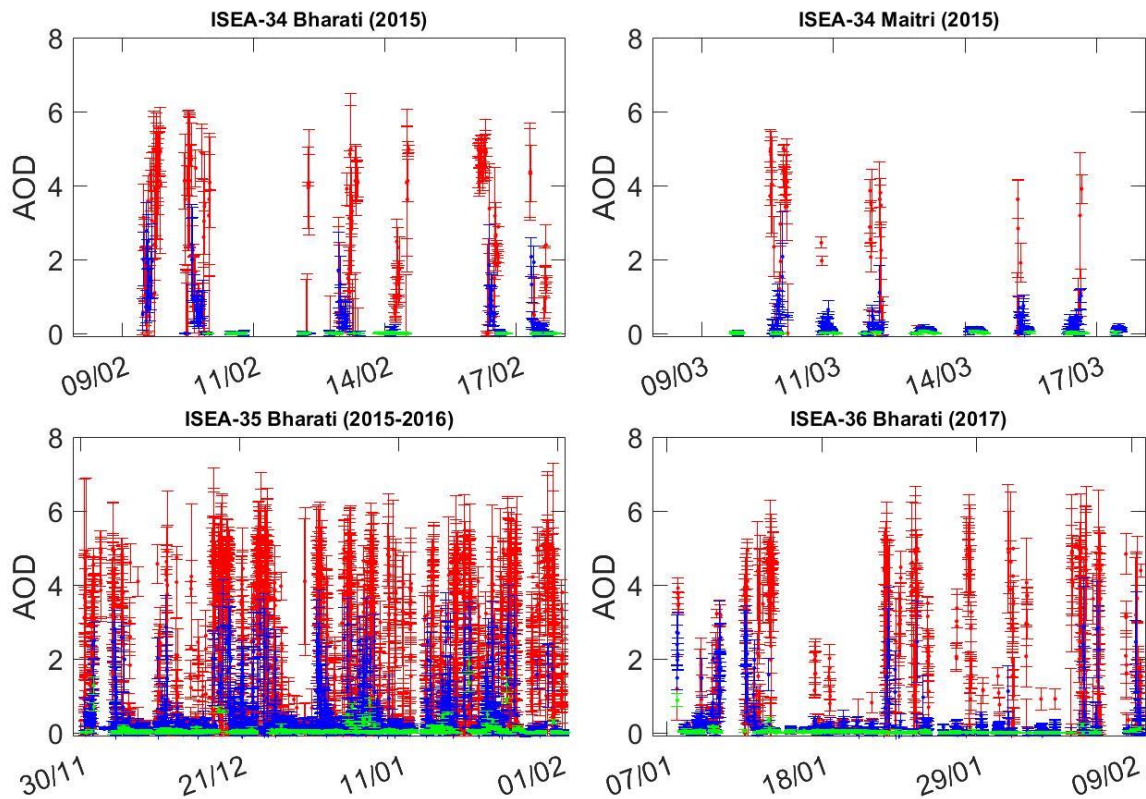


**Figure S5:** AOD timeseries retrieved using the O<sub>4</sub> DSCDs for all the four campaigns are shown. The flags for ‘good’ (green), ‘warning’ (blue) and ‘bad’ (red) are colour coded. The green data show the good datapoints, which are reliable and were mostly during clear sky conditions.

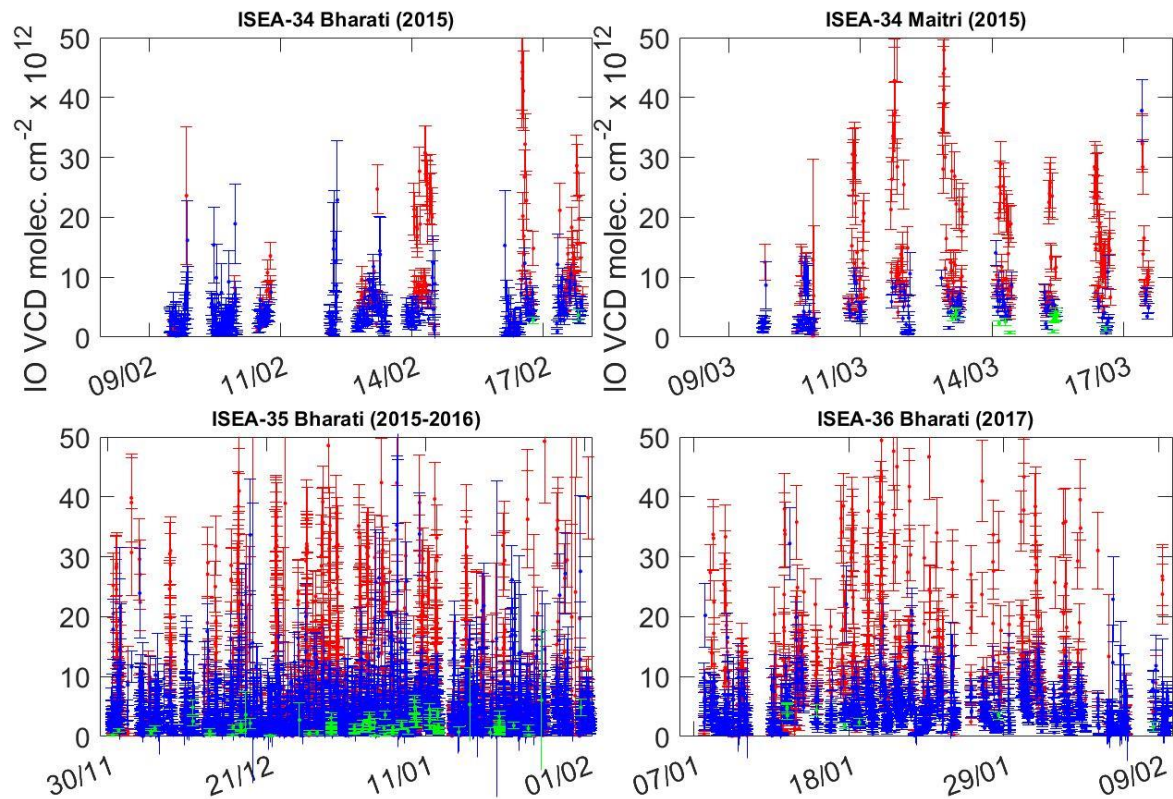
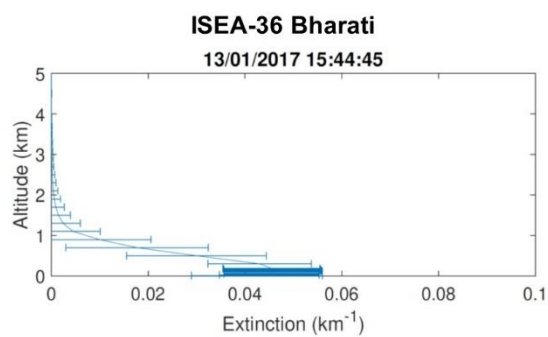
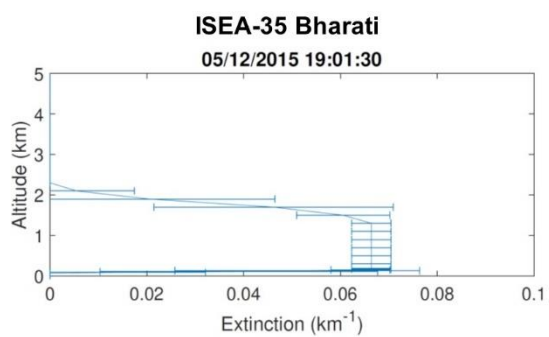
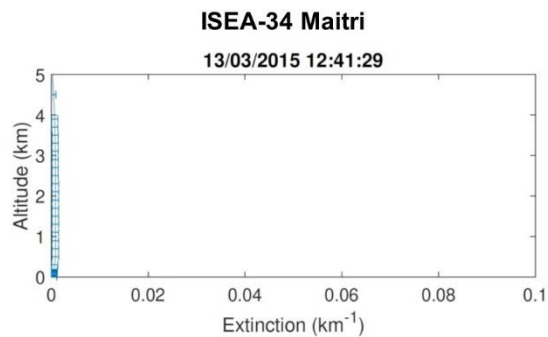
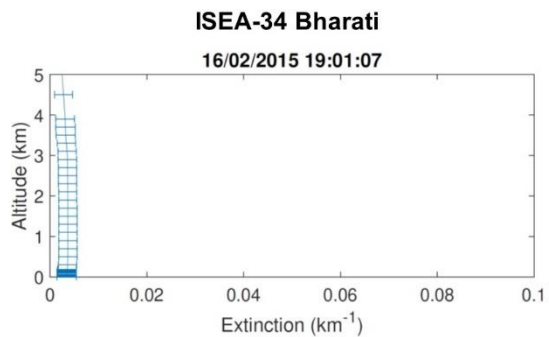


**Figure S6:** Observations of IO vertical column densities observed through all the four campaigns are shown. The flags for ‘good’ (green), ‘warning’ (blue) and ‘bad’ (red) are colour coded. These data were mostly during periods of clear sky, and where IO was observed above the detection limit for most of the set elevation angles, enabling a reliable profile retrieval.





40

41 **Figure S7:** Typical examples of aerosol extinction profiles retrieved during all the four campaigns  
 42 are shown.

43

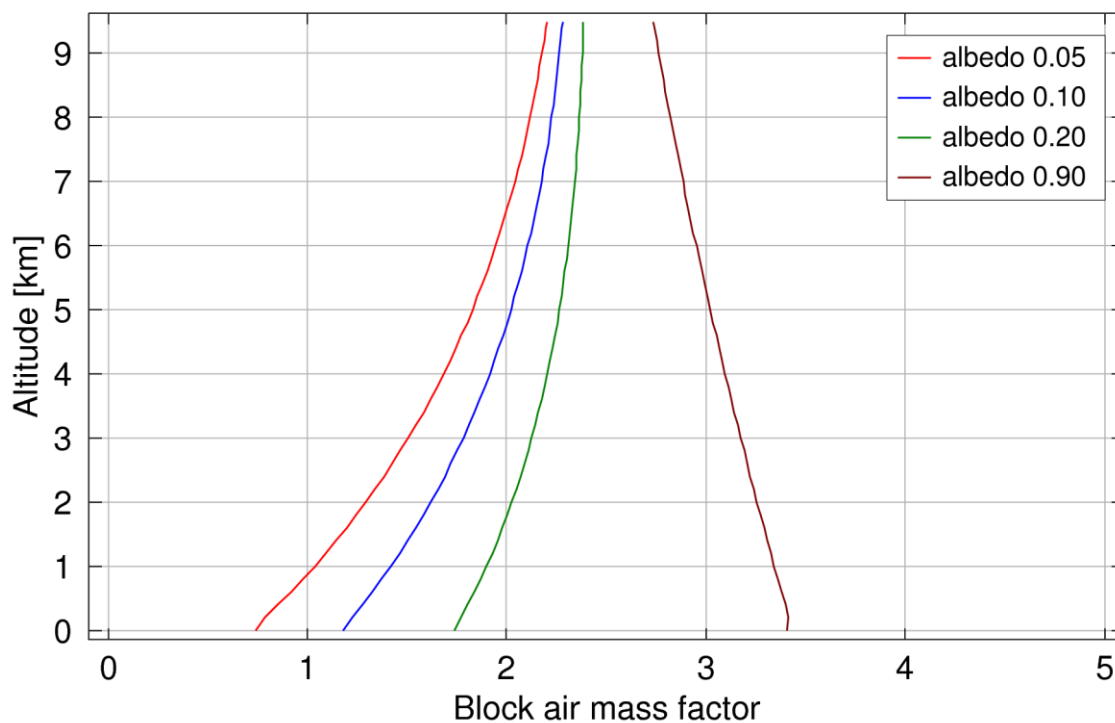
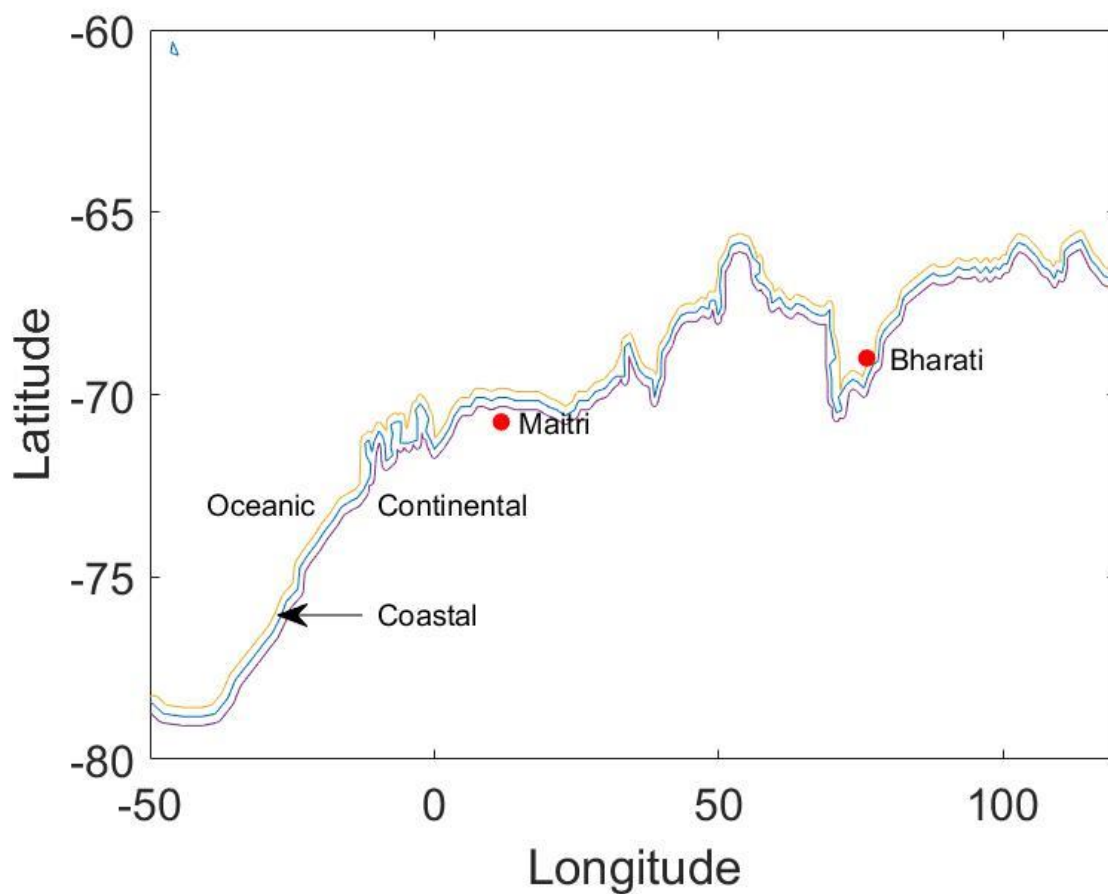


**Figure S8:** The block air mass factors for satellite retrievals showing the significant difference between the block AMFs over Antarctica at different albedo values are shown. Over the ice-covered regions in Antarctica, the satellite is sensitive to the lower troposphere as the albedo is usually 0.9 or above. However, over open ocean environments such as along the light path in Bharati, the sensitivity is much lower. Use of a higher albedo would result in an overestimation of the VCD, as is observed at Bharati.





53

54 **Figure S9:** Source regions defined for studying the back trajectories. A  $0.5^\circ$  belt along the  
 55 Antarctic coast (blue line) was selected as ‘coastal’, with the oceanic (yellow boundary) and  
 56 continental (purple boundary) defined any regions to the north and south of this belt.

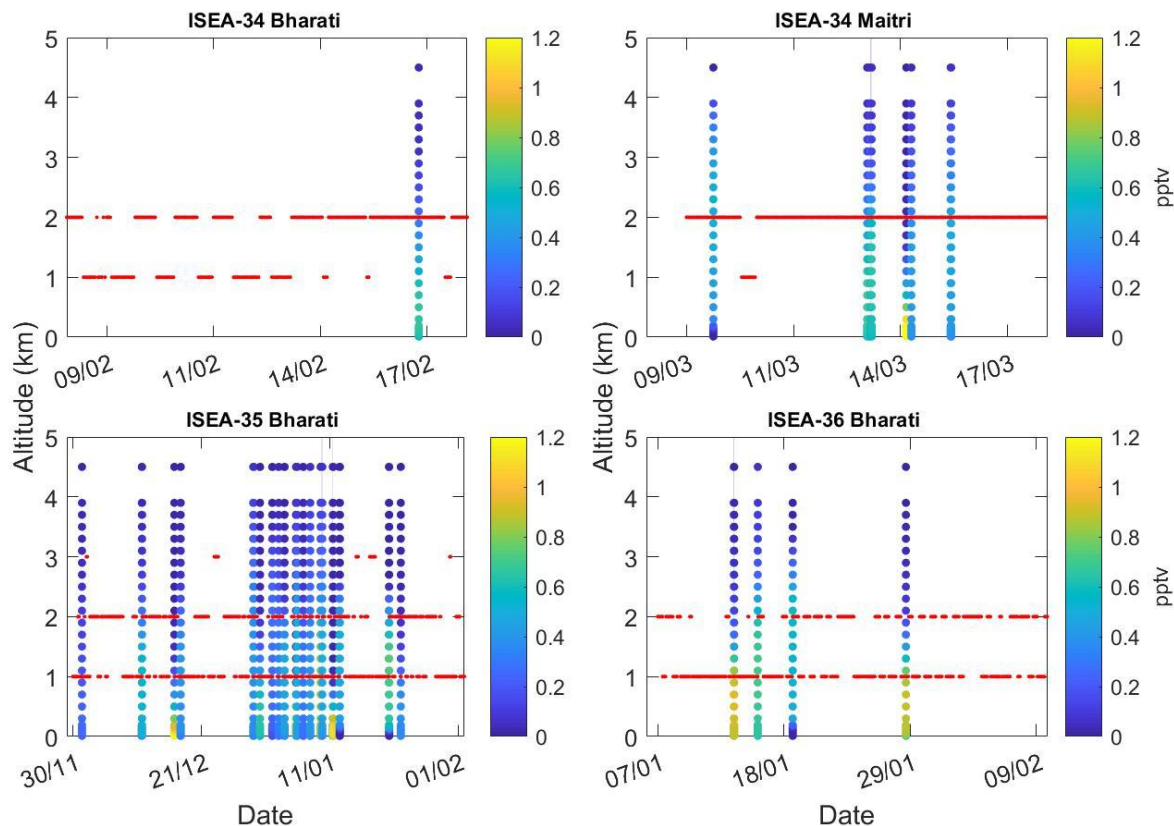


**Figure S10:** Vertical profiles of IO (coloured scatter plot) along with the source regions (red points) during all the campaigns are shown. The source regions were 1= Coastal; 2= Continental and 3= Oceanic, as defined in the text.